Received: 10 November 2023 | Revised: 19 December 2023 | Accepted: 14 January 2024

DOI: 10.1002/idm2.12146

REVIEW

Interdisciplinary Materials — Open Access — WILEY

Storage dynamics of ions on graphene

Minghao Guo | **Kun Ni** | **Yanwu Zhu**

Key Laboratory of Precision and Intelligent Chemistry, Department of Materials Science and Engineering, School of Chemistry and Materials Science, Hefei National Research Center for Physical Sciences at the Microscale, University of Science and Technology of China, Hefei, Anhui, China

Correspondence
Kun Ni and Yanwu Zhu, Key Laboratory of Precision and Intelligent Chemistry, Department of Materials Science and Engineering, School of Chemistry and Materials Science, Hefei National Research Center for Physical Sciences at the Microscale, University of Science and Technology of China, Hefei, Anhui 230026, China.
Email: nikun@ustc.edu.cn and zhuyanwu@ustc.edu.cn

Funding information
National Key Research and Development Program of China, Grant/Award Number: 2020YFA0711502; National Natural Science Foundation of China, Grant/Award Numbers: 52273234, 52273239, 52325202

Abstract

Carbon has been widely utilized as electrode in electrochemical energy storage, relying on the interaction between ions and electrode. The performance of a carbon electrode is determined by a variety of factors including the structural features of carbon material and the behavior of ions adsorbed on the carbon surface in the specific environment. As the fundamental unit of graphitic carbons, graphene has been employed as a model to understand the energy storage mechanism of carbon materials through various experimental and computational methods, ex-situ or in-situ. In this article, we provide a succinct overview of the state-of-the-art proceedings on the ion storage mechanism on graphene. Topics include the structure engineering of carbons, electric gating effect of ions, ion dynamics on the interface or in the confined space, and specifically lithium-ion storage/reaction on graphene. Our aim is to facilitate the understanding of electrochemistry on carbon electrodes.

KEYWORDS
graphene, ion dynamics, ion storage, ionic gating, nano-confinement

1 | INTRODUCTION

The intermittent nature of green energy sources and the huge demand for mobile devices/vehicles have encouraged the development of electric energy storage technique.[1,2] Electrochemical energy storage (EES) offers a promising solution due to the high energy density, high power capability, good safety and portability, among other merits.[2,3] The performance of EES is comprehensively determined by electrode materials, electrolytes, and their combination, as well as packaging and thermal management.[1] Among various electrode materials, carbons have gained a widespread attention because of high conductivity, excellent mechanical stability, and tunable surface functionality.[4] Carbons have been utilized as active materials, hosts or additives for other active materials, and current collectors.[3,5] We summarize the typical performance of some carbon nanomaterials used as supercapacitor electrodes in Table 1, including zero-dimensional (0D) carbon onions (COs) and carbon quantum dots (CQDs), one-dimensional (1D) carbon nanotubes (CNTs), two-dimensional (2D) graphene, and three-dimensional (3D) activated carbons (ACs), carbide-derived carbons (CDCs), template carbons (TCs), and carbon assemblies, for example, 3D graphene materials (3DG).

Despite the significant progress listed in the table, there remains a huge gap between the state-of-the-art and the

TABLE 1 Typical supercapacitor performances of carbon nanomaterials.[6]

Carbon	Name/type	SSA ($m^2\ g^{-1}$)	Electrolyte (mol L^{-1})	Voltage (V)	Testing conditions	Specific capacitance	References
COs	ND-1200	500	1.5 M $[NEt_4^+/BF_4^-]$/AN	2.3	5 mA cm^{-2}	38 F g^{-1}	[7]
CQDs	GQDs	–	0.5 M Na_2SO_4(aq)	1	15 μA cm^{-2}	534.7 μF cm^{-2}	[8]
CNTs	MWCNT	200	1.5 M $[NEt_4^+/BF_4^-]$/AN	2.3	5 mA cm^{-2}	18 F g^{-1}	[7]
Graphene	a-MEGO	2400	1 M $[BMIM^+/BF_4^-]$/AN	3.5	1.4 A g^{-1}	200 F g^{-1}	[9]
ACs	B-AC	2841	2 M KOH (aq)	1	1 A g^{-1}	330 F g^{-1}	[10]
CDCs	OM-CDC	2364	1 M H_2SO_4 (aq)	0.6	10 mV s^{-1}	162 F g^{-1}	[11]
TCs	Z-900	1075	0.5 M H_2SO_4 (aq)	1.2	5 mV s^{-1}	214 F g^{-1}	[12]
3DG	ZNG	2020	1 M H_2SO_4 (aq)	1	0.5 A g^{-1}	336 F g^{-1}	[13]

Abbreviations: 3DG, three-dimensional graphene materials; AC, activated carbon; aMEGO, activation of microwave exfoliated graphene oxide; AN, acetonitrile; B-AC, activated carbon obtained from Bi Luo Chun tea leaf; CDC, carbide-derived carbon; CNT, carbon nanotube; CO, carbon onion; CQD, carbon quantum dot; GQDs, graphene quantum dots; MWCNT, multiwall carbon nanotubes; OM-CDC, ordered mesoporous carbide-derived carbon; TC, template carbon; ZNG, Zn-guided three-dimensional graphene.

expected capacitance performance.[1] Purely based on the electrostatic interaction between ions and graphene, a high specific capacitance of ~550 F g^{-1}[1] could be achieved when assuming an area capacitance of ~21 μF cm^{-2},[14] for example, in ionic liquid (IL) electrolyte, and a specific surface area (SSA) of 2630 $m^2\ g^{-1}$ for graphene.[15] Further assuming an operation voltage of 4 V for the electrolyte and a density of 1.5 g cm^{-3} for 200-μm-thick graphene electrodes in a symmetric cell, an exciting energy density of 169 Wh kg^{-1} or 330 Wh L^{-1} might be obtained, superior to lead-acid batteries yet with a much faster charge/discharge process.[1] However, many factors have hampered the realization of such an excellent performance, including low SSA,[6] low density,[16] and/or low specific capacitance (e.g., 4–5 μF cm^{-2}[17]) of graphene electrodes. In addition to the regulation of quantum capacitance, which is originated from the change in Fermi level of electrons in very thin carbon electrodes due to the ion gating,[14,17] the confinement in sub-nanometer pore size shows a significant impact on the storage of ions.[18] Other factors such as space charge distribution,[19] and ion exchange/diffusion[20,21] have made the interaction between ions and electrodes illusive.[6] In observation of the complex situations that may arise in pores, a simplified research model using a "perfect" graphene electrode that can aid in understanding the fundamental interaction between carbon and ions is valuable.[20,22]

Beyond the physical adsorption of ions depicted above, the storage mechanism of metallic ions on carbon surface remains an open question,[23,24] because the staging intercalation as occurred in graphite,[25] for example, for lithium (Li) ions, may not play main roles on graphene or other carbons with high SSAs.[20] In principle, graphene can adsorb ions on both sides, yielding twice the capacity of graphite,[26] while the strong Coulombic repulsion of ions could deteriorate the adsorption.[27] The density functional theory (DFT) calculation shows that perfect graphene is unfavorable to Li storage[28] due to the weak adsorption energy (~0.190 eV vs. Li^+/Li metal).[29] Defects in graphene like vacancy, however, would lead to a higher adsorption energy and thus trap ions for enhanced storage.[20,28] In addition to the first-layer adsorption on the basal plane, a close packing of Li has been observed in the confined space in bilayer graphene, resulting in a higher Li storage capacity.[23] More importantly, but has not been often noticed, the Li adsorption/desorption may cause the development of defects, leading to a continuous structural deterioration of graphene during the electrochemical cycling.[20]

Clearly, even a simplified graphene model deserves more research attention as a scenario for ion dynamic research. The complex factors remain, including but not limited to the structural feature of the graphene electrode itself and those coming from the interaction between ions and graphene in the specific electrochemical measurement. In this review, we would provide a concise overview of recent proceedings on the ion storage for graphene-based materials. By discussing the structural modulation strategies, ionic gating effects, ion behaviors at interface or in confined space, and lithium-ion storage mechanisms on graphene, we hope that the understanding of carbon electrode for EES is promoted.

2 | STRUCTURAL MODULATION OF GRAPHENE MATERIALS

In the pursuit of enhancing SSA of graphene materials, Zhu et al. reported a 3D porous carbon made by chemical activation of microwave exfoliated graphene oxide (aMEGO)

with KOH, which demonstrates a SSA of 3100 $m^2 g^{-1}$ and a specific capacitance of 200 $F g^{-1}$ in neat ethyl-methyl-imidazolium bis(trifluormethylsulfonyl)imide ($EMIM^+$/$TFSI^-$).[9] However, the volume capacitance of obtained aMEGO carbon is very low due to the low density (~0.35 g cm^{-3}), restricting the performance of practical devices.[16] Upon a simple mechanical compression, the width of mesopores in aMEGO at ~2 nm was narrowed, while the pores with ~1 nm width maintain the size,[16] as shown in Figure 1A. The density increases from 0.34 to 0.61 g cm^{-3} under a force of 10 tons.[16] Therefore, compressing aMEGO has substantially enhanced the volumetric capacitance and energy density to 110 F cm^{-3} and 48 Wh L^{-1} in 1-butyl-3-methyl-imidazolium tetrafluoroborate dissolved in acetonitrile [$BMIM^+/BF_4^-$]/AN electrolyte, from originally 54 F cm^{-3} and 23 Wh L^{-1}.[16] In another work, by performing the KOH activation of graphene oxide (GO) in a sponge template, the volumetric capacitance has been further improved to 149 F cm^{-3} in butyl-3-methyl-imidazolium hexafluorophosphate dissolved in acetonitrile [$BMIM^+/PF^{6-}$])/AN,[31] indicating the promising role of regulating the structure of graphene electrodes for the higher volumetric performances.

Because the total capacitance is a series connection of electrical double layer (EDL) capacitance and quantum capacitance, the structural defects could make changes to total capacitance, as the defect may affect the quantum capacitance by changing the electronic states.[4,30] In addition, the formation of nanoscale defects would provide extra channels for the ion diffusion.[21,32] Defects, such as topological defects,[30] dangling-bond-rich vacancy defects,[33] and big holes,[21] have been created by Ar^+ plasma etching, as shown in Figure 1B,C. Few-layer graphene (FLG) made by chemical vapor deposition (CVD) in benzylamine and acetonitrile was etched by Ar^+ plasma treatment, based on which the capacitance in tetraethylammonium tetrafluoroborate/acetonitrile ([TEA^+/BF_4^-]/AN) or tetrabutylammonium hexafluorophosphate/acetonitrile ([TBA^+/PF_6^-]/AN) has been increased,[21] as shown in Figure 1D. The number of defects was quantified by the I_D/I_G of Raman spectra (inset of Figure 1D). Previous studies have shown that H_2O_2 produces hydroxyl radicals, which attack the carbon–carbon bonds of graphene, resulting in the etching and oxidation; infrared absorption spectroscopy confirms the higher absorption from hydroxyl and carbonyl groups.[34] By H_2O_2 treatment, Xu et al. reported enhanced accessible area of graphene electrode with better ion transportation, thus achieving high volumetric capacitance (212 F cm^{-3}) while maintaining the high gravimetric capacitance (298 F g^{-1}), high energy density (127 Wh kg^{-1}), and excellent rate performance, when tested at 1 A g^{-1} in 1-ethyl-3-methylimidazolium tetrafluoroborate/acetonitrile ([$EMIM^+/BF_4^-$]/AN) electrolyte.[32]

Doping with heteroatoms,[4] as demonstrated in Figure 1E, can increase the density of states (DOS) at the Fermi level by introducing a localized dopant state like phosphorus,[35] or by moving the Fermi level upward or downward with, for example, boron doping,[36] nitrogen doping,[30] fluorine doping,[37] or sulfur doping.[38] Since the total capacitance (C_{total}) can be regarded as the serial combination of double-layer capacitance (C_{EDL}) and quantum capacitance (C_Q), given by ${C_{total}}^{-1} = {C_{EDL}}^{-1} + {C_Q}^{-1}$, and C_Q is sensitive to the density of states at the Fermi level (DOS_{EF}) by $C_Q = e^2 DOS_{EF}$,[4,30] doping can modify the quantum capacitance and make changes to the total capacitance.[30] The higher electronegativity of nitrogen (3.04), compared with carbon (2.55), leading to the spontaneous charge transfer from nitrogen to carbon when nitrogen is doped into carbon lattice, which could benefit the adsorption of ions.[39] Lee et al. reported that the capacitance of reduced graphene oxide (rGO) can be increased to 218 from 189.6 F g^{-1} by pyridine and pyrrole nitrogen doping in 1 M H_2SO_4 electrolytes.[40] Nitrogen dopant can also promote the ion transport in graphene.[41] Pham et al. observed that N-doped graphene (3.5 at.%) produced by arc-discharge plasma exhibited a relaxation time reduction by 50% compared with pristine graphene, measured by electrochemical impedance spectroscopy.[41] Sulfur doping creates an extended π system by overlapping the p orbitals of sulfur and carbon atoms, thereby enhancing the conductivity and leading to improved polarization and higher capacitance.[42] Wu et al. reported sulfur-doped graphene-based micro-supercapacitors with higher electrical conductivity (~95 S cm^{-1}) and volume capacitance (~582 F cm^{-3}) in H_2SO_4/poly(vinyl alcohol) (H_2SO_4/PVA) gel electrolyte, compared with rGO (~245 F cm^{-3}).[43] The oxygen doping in the forms of C–O–C, C–OH or C=O groups has been introduced to increase the surface wettability and ion diffusion rate, leading to an enhanced charge transfer rate of ions, but the electron conductivity may be reduced.[39] Sruthi et al. have shown that the quantum capacitance increased from 20.0 to 247.4 $\mu F\ cm^{-2}$ by varying O/C ratio from 0.02 to 0.39 in oxidized graphene based on DFT simulations.[44]

The capacitance at the interface between graphene and electrolyte contains Helmholtz layer capacitance on the electrolyte side and the space charge capacitance inside the electrode, which is largely affected by the charge distribution in the electrode and the corresponding screening effect.[19,45] By stacking graphene with specific number of layers, Wang et al. reported 3-4 times increase of screening length, inversely proportional to the space charge capacitance, when the thickness is increased by 5–45 times from graphene to graphite.[19] For thin electrodes, the quantum capacitance becomes a crucial factor for total capacitance.[46] Ji et al. reported

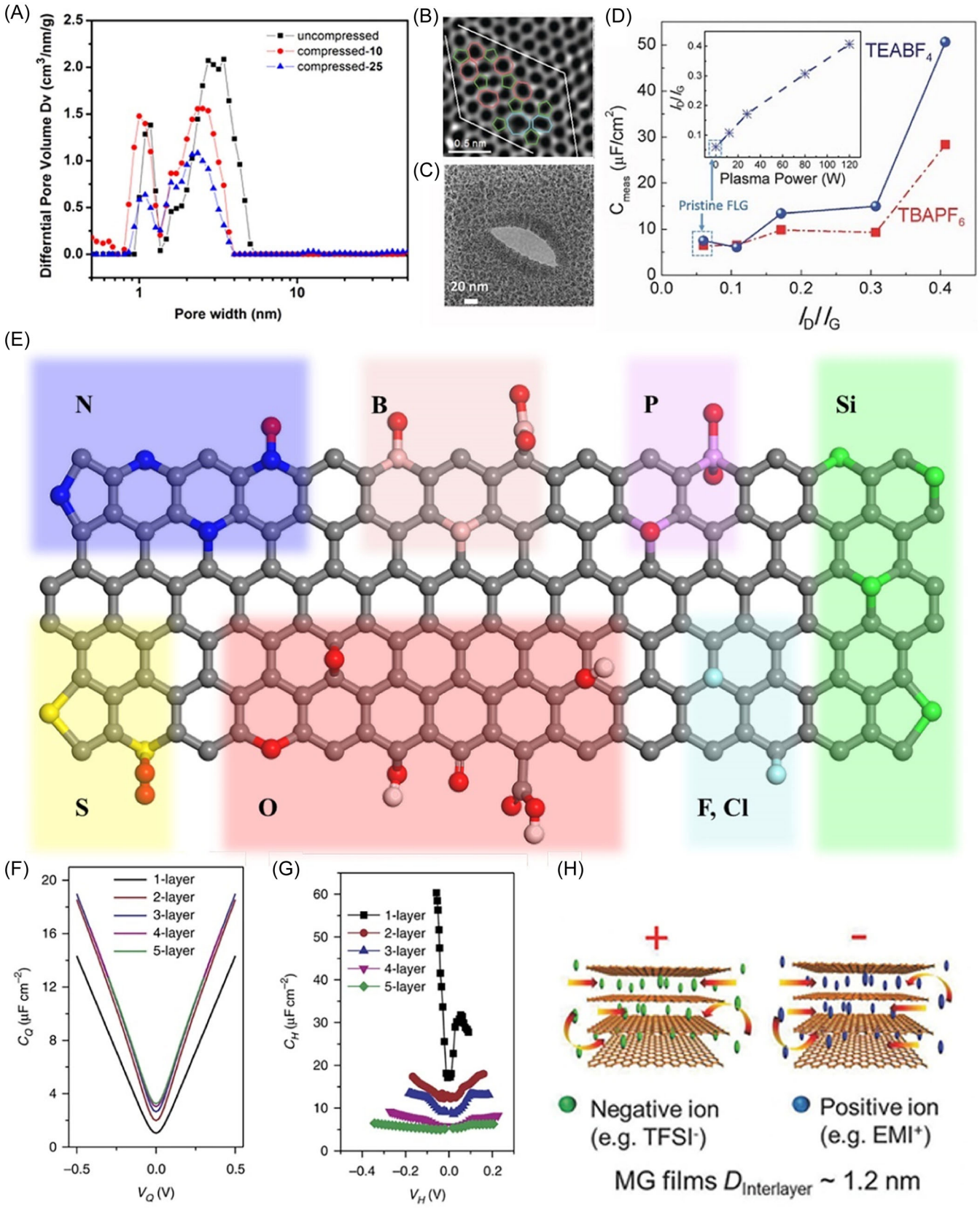

FIGURE 1 (See caption on next page).

the increased quantum capacitance of graphene in 6 M KOH solution with the increased number of layers[17] (Figure 1F). The increased quantum capacitance is attributed to the increased DOS in FLG compared with single layer graphene (SLG), and the accumulation of space charge near the solid/electrolyte interface.[17] As shown in Figure 1G, the interface capacitance and the slope of interface capacitance vs voltage simultaneously increases when decreasing the layer numbers, indicating the stronger electron–ion interaction between SLG and electrolyte.[17]

When a graphene film is exposed to the electrolyte, most of accessible area may contribute to the charge storage,[21] raising a question of competence between ions. Ye et al. investigated the layer dependence of the capacitance of FLG micro-capacitor, which is prepared by direct laser writing on CVD graphene.[47] The number of layers was controlled by a repeated sequential dry transfer process with the interlayer space (~1.2 nm) accessible for ions, as schematically shown in Figure 1H.[47] The specific capacitance in $EMIM^+/TFSI^-$ electrolyte decreases from 52 to 32 $\mu F\,cm^{-2}$ as the number of layers keep increasing from 2 to 8, surpassing the reported intrinsic capacitance of ~21 $\mu F\,cm^{-2}$.[14,47] The charge density on the 8-layer graphene was calculated as 0.012 e $Å^{-2}$, lower than the theoretical maximum charge density of 0.031 e $Å^{-2}$ for $TFSI^-$ or 0.044 e $Å^{-2}$ for EMI^+, by assuming a close packing of ions on the graphene.[47] The results suggest that the charge storage on graphene might be further optimized by increasing the accessible area of electrode.

3 | ELECTROSTATIC AND IONIC GATING EFFECT

Measuring the carrier concentration in the electrode and the ionic dynamics at the electrolyte interface are basic for understanding factors influencing EES.[48] Ionic gating is a feasible way to induce a substantial charge accumulation and create a local electric field on the graphene/electrolyte interface,[49] as typically shown in Figure 2A. By applying a gate voltage, the Fermi level and the carrier density in graphene could be effectively controlled.[49] As graphene is an ambipolar electrode material, the doping type and strength can be tuned both positively and negatively (Figure 2B), which can be measured by in-situ Raman spectroscopy.[50] Das et al. observed an ultrahigh electron doping of up to $5 \times 10^{13}\,cm^{-2}$ for graphene in polyethylene oxide/$LiClO_4$ ($PEO/LiClO_4$) electrolyte, which is much higher than the value that the electrostatic gating effect can achieve.[50] Figure 2C rationalizes the doping strength by the intensity ratio of 2D to G peak.[50] In polyethylene glycol/$NaClO_4$ ($PEG/NaClO_4$) electrolyte, Mafra et al. observed that applying a gate voltage disrupts the inversion symmetry in bilayer graphene due to the different charge carrier concentrations in two layers, and thus the G band splits into two modes representing E_g and E_u of the D_{3d} point group.[53] Such a gate voltage can also induce an energy difference of electrons between two layers of bilayer graphene, leading to the formation of bandgap.[54] Mak et al. showed that the ionic top gate resulted in the formation of a bandgap about 200 meV in bilayer graphene, as shown in the green curve in Figure 2D.[51]

Ionic gating has been applied to modulate the quantum capacitance of graphene. In 2009, Xia et al. measured the quantum capacitance of mechanically exfoliated SLG exposed to $BMIM^+/PF_6^-$ electrolyte.[17] The interface capacitance of graphene was measured to be 21 $\mu F\,cm^{-2}$ and the quantum capacitance measured was linearly dependent on the bias potential, agreeing with theoretical calculations.[17] When a nanoporous membrane made from rGO was used as the work electrode in 1.0 M KCl electrolyte (Figure 2E), Xiao et al. observed that the conductance across the membrane changed non-monotonically with the gate potential from 0 to 0.8 V, showing a minimum value at 0.6 V, and the potential dependency of the conductance has been attributed to the regulation of the DOS at Fermi level of rGO electrode.[48]

FIGURE 1 (A) Pore width distribution of uncompressed and compressed activation of microwave exfoliated graphene oxide (compression force of 10 or 25 tons) measured by N_2 adsorption with the slit/cylindrical nonlocal density functional theory model.[16] (B) Topological defects in single layer graphene[30] and (C) extended pores in few-layer graphene (FLG)[21] caused by Ar^+ plasma treatment, observed by transmission electron microscopy. (D) Relationship between specific capacitance and intensity ratio between D peak and G peak (I_D/I_G) of Raman spectra in FLG. Inset shows the increased I_D/I_G with increasing plasma power.[21] (E) Heteroatom doping in graphene. (F) Quantum capacitance and (G) Helmholtz capacitance versus voltage in 6 M KOH aqueous solution depending on number of layers in multilayer graphene (MLG).[17] (H) Schematic diagram of ion intercalation in MLG.[31] (A) Reproduced with permission.[16] Copyright 2013, Elsevier. (B) Reproduced with permission.[30] Copyright 2016, Wiley-VCH. (C, D) Reproduced with permission.[21] Copyright 2016, Wiley-VCH. (F, G) Reproduced under the terms of the CC-BY Creative Commons Attribution 4.0 International License.[17] Copyright 2014, Springer Nature. (H) Reproduced with permission.[31] Copyright 2018, Wiley-VCH.

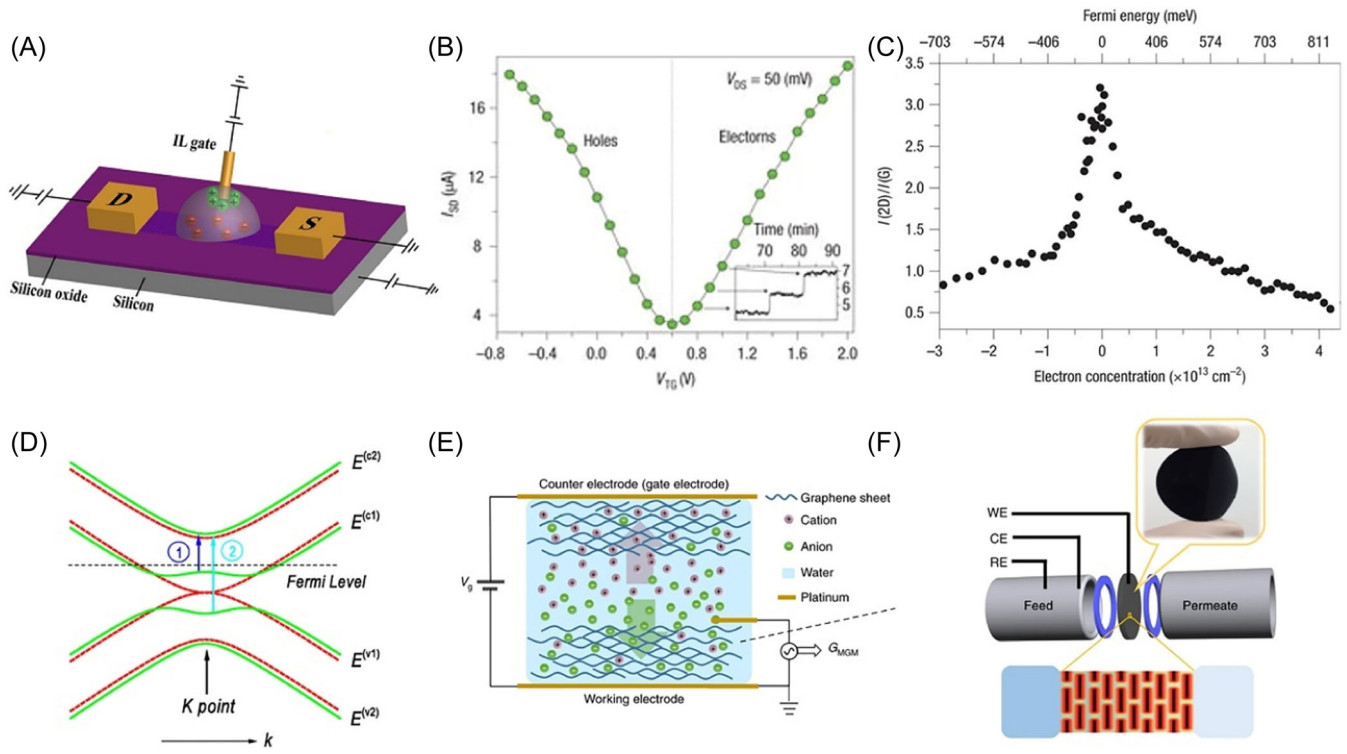

FIGURE 2 (A) Device of an IL gated graphene.[49] (B) Current through source and drain modulated by the gate voltage in PEO/$LiClO_4$ electrolyte.[50] (C) Ratio of 2D to G Raman peak intensity of graphene in PEO/$LiClO_4$ electrolyte.[50] (D) Band structure of bilayer graphene before (red) and after (green) applying a perpendicular electric field based on the tight-binding model calculation.[51] (E) Schematic diagram of IL-gated graphene membrane in KCl aqueous solution.[48] (F) Real-time permeation monitoring device of the rGO membrane in 1.0 M KCl aqueous solution.[52] (A) Reproduced with permission.[49] Copyright 2014, IOP Publishing. (B, C) Reproduced under the terms of the CC-BY Creative Commons Attribution 4.0 International License.[50] Copyright 2008, Springer Nature. (D) Reproduced with permission.[51] Copyright 2009, APS Publishing. (E) Reproduced under the terms of the CC-BY Creative Commons Attribution 4.0 International License.[48] Copyright 2020, Springer Nature. (F) Reproduced under the terms of the CC-BY Creative Commons Attribution 4.0 International License.[52] Copyright 2018, Springer Nature. IL, ionic liquid; rGO, reduced graphene oxide.

The ionic gating effect can also regulate the permeation of ions through the basal plane of graphene. In 2018, Cheng et al. conducted experiments to verify the gating effect on permeation of ions by using a three-electrode device, consisting of a rGO membrane as work electrode in 0.1 M KCl aqueous solution, as depicted in Figure 2F.[52] It was observed that the ion diffusion between the layer with a spacing less than 2 nm is significantly enhanced under gate voltage within ±0.5 V, which is 4–7 times faster than the theoretical prediction without gating effect, further verified by the Poisson–Nernst–Planck (PNP) modeling simulation.[52] Distinct ion behavior is observed when the pore size is further reduced. Using the device shown in Figure 2E, for the interlayer distance less than 1 nm, an ionic hysteresis was observed in 1.0 M $BMIM^+/BF_4^-$ aqueous solution, neat IL $EMIM^+/BF_4^-$ or $K^+/TFSI^-$, attributed to the slow ionic dynamics caused by the limited mobility of ions and ion reorganization at the electrolyte/electrode interface.[48]

4 | ION ADSORPTION AT GRAPHENE–ELECTROLYTE INTERFACE

The electrochemistry at the graphene-electrolyte interface involves the transport of ions through electrode channels, as well as the adsorption and desorption of ions.[22] Due to the Coulombic interaction, the ions with opposite charges form the alternate arrangement, which is known as Coulombic ordering.[55] Previous study shows that counter-ion adsorption and ion-exchange (counter-ion adsorption with co-ion desorption) occurs to rebuild the ion ordering in different stage of polarization, due to the spatial confinement effect in nanopores.[56] To investigate the EDL structure while minimizing the influence of quantum capacitance, Ye et al. measured the mass change (Δm) of neat IL $EMIM^+/TFSI^-$ on SLG electrode by an electrochemical quartz crystal microbalance (EQCM).[22] Δm could be calculated by Sauerbrey's equation, $\Delta m = C_f \times \Delta f$, where Δf is the frequency change of the

quartz and C_f is the sensitive factor of the quartz.[56] As shown in Figure 3A, the mass of the electrode decreases with positive polarization, with a changing rate of 338 g mol^{-1}, corresponding to a normalized chemical formula of $[EMIM_{1.58}TFSI_{0.58}]^+$.[22] Under negative polarization, however, an ion redistribution at the interface has been observed, showing no significant mass change, which is further confirmed by molecular dynamics simulations.[22] Different from the situation of neat IL, the presence of solvent with high dielectric constant, for example, AN, may reduce the screening length of ions and the EDL thickness.[60] Wu et al. observed that SLG in 2 M [EMIM$^+$/TFSI$^-$]/AN electrolyte has the higher charge carrier density at the interface than the situation in the neat EMIM$^+$/TFSI$^-$, especially from the potential of zero charge to negative polarization.[57] As depicted in Figure 3B, the results of EQCM reveal an increase in the weight of the electrode under both positive and negative polarization.[57] The change of weight per mole charge was 325 g mol^{-1} ($[TFSI_1AN_{1.3}]^-$) for positive polarization and 152 g mol^{-1} ($[EMIM_1AN_1]^+$) for negative polarization, showing fewer AN molecules in the solvent shell of ions compared with the situation in carbon micropores, which has three to four AN molecules.[57]

The geometry of IL molecules largely affects the structure of EDL.[61] In most cases, IL without a long alkyl tail exhibits an over-screening effect at low or zero potential, but shows an over-crowded effect at high polarization potential with increased thickness of EDL and decreased capacitance.[61] For IL with a long alkyl tail, on the other hand, non-polarized tails occupy the position available for other charge at low polarization potential or

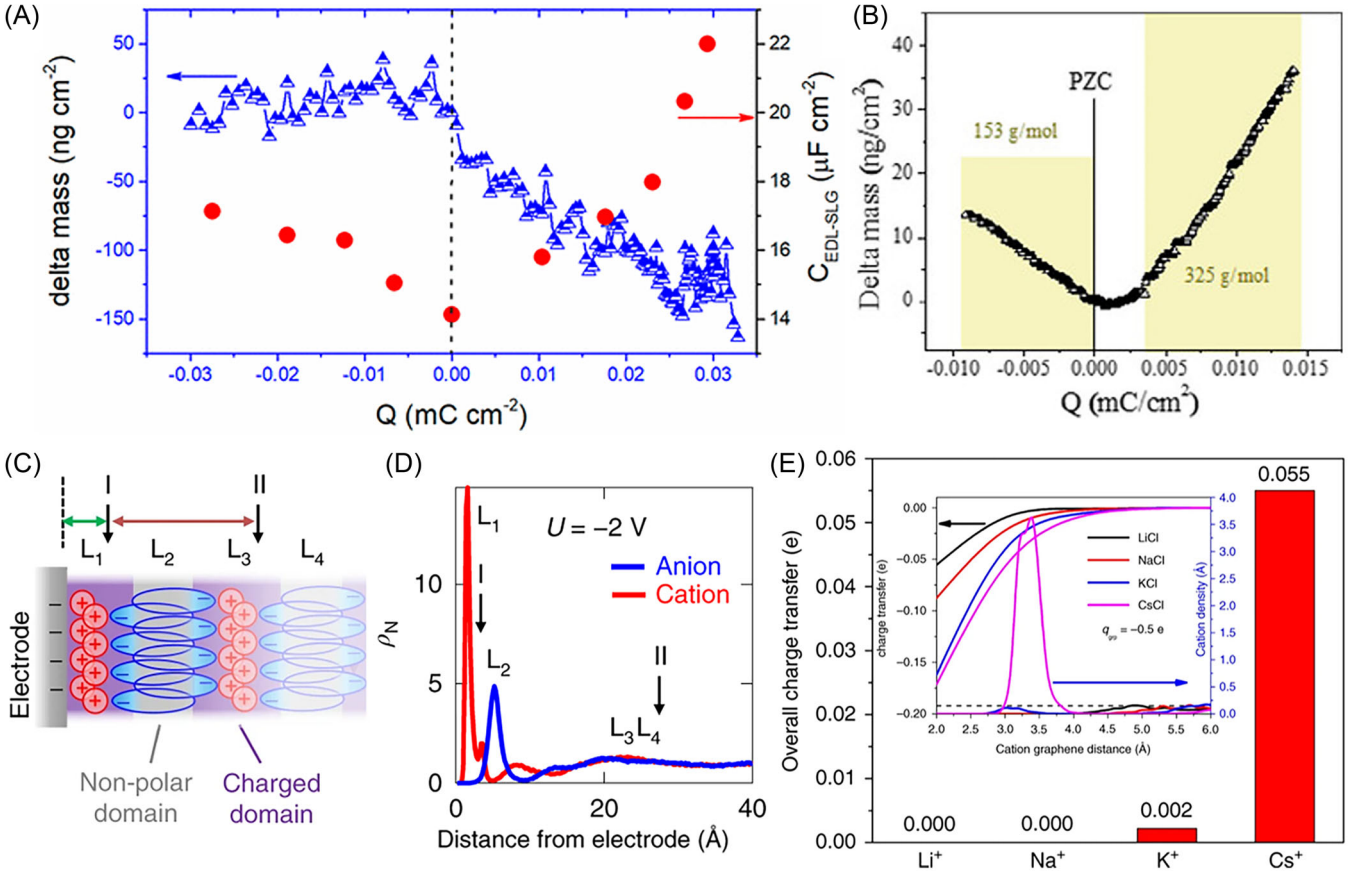

FIGURE 3 (A) Change of mass and double layer capacitance measured on SLG in pure EMI$^+$/TFSI.[22] (B) Change of mass on SLG in 2 M [EMIM$^+$/TFSI$^-$]/AN electrolyte.[57] (C) Ion arrangement and (D) ion number density of $C_4C_1Im^+$/AOT$^-$ at the charged graphitic interface simulated by molecular dynamics.[58] (E) The total charge transfer from hydrated cations to graphene electrode in 1.00 M LiCl, NaCl, KCl, CsCl aqueous solution calculated by integrating the charge transfer per ion and the local cation density, derived from the Boltzmann weight of the potential energy surface on graphene electrode, both in the inset.[59] (A) Reproduced with permission.[22] Copyright 2019, American Chemical Society. (B) Reproduced with permission.[57] Copyright 2021, Wiley-VCH. (C, D) Reproduced under the terms of the CC-BY Creative Commons Attribution 4.0 International License.[58] Copyright 2019, Springer Nature. (E) Reproduced under the terms of the CC-BY Creative Commons Attribution 4.0 International License.[59] Copyright 2019, Springer Nature. SLG, single layer graphene.

zero potential[62] and increase the negative potential for over-crowed effect by decreasing the amount of charge.[63] As an example, Mao et al. have proposed an amphiphilic IL, 1-butyl-3-methylimidazolium/1,4-bis(2-ethylhexoxy)-1,4-dioxobutane-2-sulfonate ($C_4C_1Im^+/AOT^-$), with an amphiphilic anion (AOT^-) consisting of a negative polar head and an alkyl non-polar tail, which is distinct from the non-amphiphilic IL $EMIM^+/TFSI^-$, resulting in a capacitance of ~234 F g^{-1} at a scan rate of 10 mV s^{-1} at 200°C.[58] Molecular dynamics simulations illustrate two alternating charge layers consisting of polar domain constructed by negative polar head of $AOT^-$and positive $C_4C_1Im^+$, and the non-polar domain constructed by non-polar tail of AOT^- formed the interface for 2 and −2 V,[58] as shown in Figure 3C. The introduction of non-polar domain by alkyl non-polar tails of amphiphilic IL causes the decrease of the over-screening effect of adsorbed ions, leading to increased density of counter ions in the first adsorption layer,[58] as shown in Figure 3D.

In addition to the study of organic ILs, the investigation of aqueous salt solutions at graphene interface has gained significant attention.[64] The classical molecular dynamic simulations, which assume that the ions are point charges, predict that the larger ions have a longer distance from graphene and lower capacitance, which however is contradictory to the experimental observation of increased capacitance for the larger ion size.[65] To address this issue, Zhan et al. employed DFT calculations in combination with the reference interaction site model to elucidate the impact of electrons, to investigate the adsorption behavior of solvated alkali metal ions at the graphene interface.[59] Consistent with the adsorption sequence ($Cs^+ > K^+ > Na^+ > Li^+$) of the cations on the charged interface in 1.00 M LiCl, NaCl, KCl, CsCl solutions, larger cations have weaker and smaller solvation shells, which facilitate their de-solvation and adsorption on the electrode.[59,66] Furthermore, the larger ion exhibit greater polarizability and more significant charge transfer with graphene, as shown in Figure 3E.[59] Considering the local cation density on the electrode in the inset of Figure 3E and the charge transfer of the single ion, the overall charge storage capacity of larger ion would be higher.[59]

5 | ION DYNAMICS IN CONFINED SPACE

The development of a unified theory that could explain the relationship between the pore structure and the capacitance is challenging.[6,67–69]. Galhena et al. showed that the capacitance increases anomalously when the pore size approaches the size of desolvated ion.[70] Fluids within space with at least one characteristic dimension below 100 nm may exhibit phenomena different from those at the macroscopic scale are referred to as nanofluidics.[71] The interlayer space in 2D materials, through the confinement effect on ions and solvents, alters the behavior of ions within as-formed 2D nanofluidics.[72] Especially, when the interlayer spacing is smaller than the Debye length of ions, ions with charges opposite to the walls become the preferred charge carriers, leading to several orders of magnitude increase in ionic conductivity, for example, in GO slits.[72] Further studies have shown that the confined space has a significant impact on the behavior of ions, and the charged walls of the confinement could greatly enhance the ion diffusion and transportation at low ion concentration.[73]

For GO films, the interlayer distance can be influenced by the humidity,[74] till an interlayer distance of ~13.5 Å. Many strategies, such as partial reduction,[75] covalent crosslinking,[76] physical confinement,[77] and cation treatment,[78] have been proposed to reduce the interlayer distance. Chen et al. reported that the interlayer spacing of partially oxidized graphene laminate films can be precisely adjusted by treating with various cations, and K^+ induces the minimum interlayer distance of ~11 Å (Figure 4A).[78] The DFT simulations suggest the repulsion energy between K^+ , and the GO membrane is equal to the hydration energy, indicating that the hydration structure of K^+ in GO is unstable.[78] Therefore, the distortion of K^+ hydrated structure inside GO membrane may reduce the interlayer distance. Esfandiar et al. reported the preparation of angstrom-scale slits by stacking bilayer graphene in the middle of two bulk graphite.[79] As shown in Figure 4B, the mobility ratio of cations to Cl^- is reduced by 90% with increased hydration radius from K^+ to Al^{3+}.[79] The mobility of Cl^- is reduced by 75% compared with that of bulk solution, while K^+ is unaffected, due to the stronger interaction between Cl^- and graphene.[79] Li et al. mixed GO and exfoliated graphene in water and obtained the membrane by vacuum filtration.[18] The pore size distribution of the obtained membrane has been precisely controlled by the content of exfoliated graphene in the mixture suspension,[18] as shown in Figure 4C. When the pore size matches the diameter of electrolyte ions, the utilization of pores becomes the highest, resulting in a good balance between porosity and density, yielding an optimal capacitance, indicated by the volumetric capacitance of 203 F cm^{-3} at a bulk density of 0.94 g cm^{-3}.[18]

MLG is considered to contain the confined space for ion transport, particularly for ions that tend to intercalate,

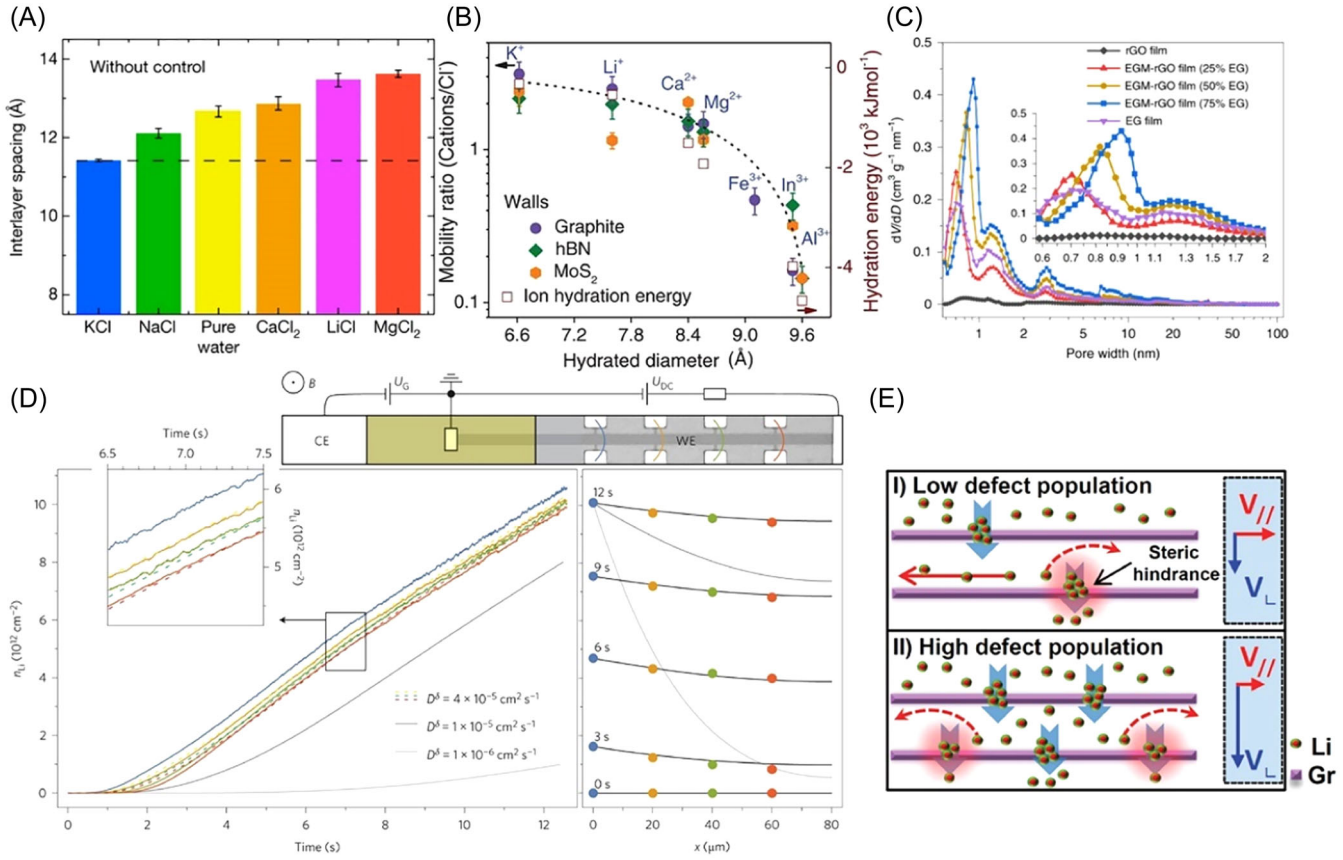

FIGURE 4 (A) Interlayer spacing of GO membrane treated by water or 0.25 M salt aqueous solution.[78] (B) Mobility of different ions in angstrom-scale slit constructed by pushing two pieces of bulk graphite, hBN and MoS_2 together.[79] (C) Pore-size distribution of graphene membrane depending on the content of exfoliated graphene.[18] (D) Li concentration n_{Li} versus time extracted at four positions (blue, yellow, green, and red) on the bilayer graphene shown in the upper panel under $B = 10$ T and $T = 300$ K, and the fitting slope gives the diffusion constant of Li^+ in bilayer graphene. The right panel shows the Li density at different positions on the bilayer graphene at different time.[80] (E) Diffusion pathway of Li^+ in low and high defect density in MLG.[81] (A) Reproduced under the terms of the CC-BY Creative Commons Attribution 4.0 International License.[78] Copyright 2017, Springer Nature. (B) Reproduced with permission.[79] Copyright 2017, American Association for the Advancement of Science. (C) Reproduced under the terms of the CC-BY Creative Commons Attribution 4.0 International License.[18] Copyright 2020, Springer Nature. (D) Reproduced under the terms of the CC-BY Creative Commons Attribution 4.0 International License.[80] Copyright 2017, Springer Nature. (E) Reproduced with permission.[81] Copyright 2012, American Chemical Society. MLG, multilayer graphene.

such as Li^+. Kuehne et al. designed an in-situ electrochemical device, using a mechanically exfoliated bilayer graphene Hall bar as the working electrode.[80] Notably, in the bilayer graphene sample, upper layer only covers the center part of the bottom layer, and the immobilization reaction product caused by Li insertion only occurs at the edge of the upper layer graphene, rather than on the uncovered part of the bottom graphene, indicating that Li^+ mainly diffuses through the interlayer of graphene.[80] The in-plane Li^+ diffusion coefficient was measured to be $7 \times 10^{-5}\,cm^2\,s^{-1}$,[80] as shown in Figure 4D. Yao et al. proposed a defect-assisted Li diffusion mechanism in MLG,[81] in which Li^+ diffuses along the graphene plane till a trap by defects, then penetrates the plane through defects with a lower diffusion barrier (2.36 eV for divacancy), as shown in Figure 4E. In fact, Li^+ penetration through pristine graphene is almost impossible because of the high energy barrier of ~10.2 eV.[81]

6 | CHARGE TRANSFER BETWEEN LITHIUM IONS AND GRAPHENE

The interaction between Li atoms and graphene varies among covalency, ionicity, and metallicity, corresponding to the different Li storage mechanisms on graphene.[25] A theoretical arrangement of Li atoms on both sides of graphene yields a capacity of 744 mAh g^{-1}, but the binding energy would decrease due to the strong

Coulombic repulsion between Li atoms on opposite sides once the surface coverage exceeds 5%, based on DFT simulations.[27] In addition, the low nucleation overpotential (~ −33.2 mV) of Li on graphene results in the Li plating on graphene exposed to electrolyte, providing a potential high-SSA substrate for uniform Li metal storage by modulating lithiophilicity.[82] Chen et al. considered various doping elements and doping types in graphene and found that the dopants generating negatively charged adsorption sites and strong local dipoles, like nitrogen, oxygen, and boron, were found to be more favorable to heterogeneous Li nucleation, thus reducing the nucleation barrier.[83] As shown in Figure 5A, Zhang et al. treated GO at low temperature in vacuum and then in ammonia at 600°C, promoting a lithiophilicity by nitrogen dopant.[84] After plating of Li at 0.05 mA cm^{-2}, a flat metallic deposition was formed on the nitrogen-doped graphene, in contrast to the dendrite on copper (Cu) surface.[84]

The Li stored on graphene is not a body-centered cubic metal, but a face-centered cubic or hexagon structure.[20,23,85,86] Li et al. investigated the role of graphene in guiding Li deposition, by immersing a Cu foil in a GO solution.[85] X-ray diffraction measurements revealed that the deposited lithium has 71% (110) facet on the rGO, while that of Cu foil was 40%.[85] As shown in Figure 5B, the lattice mismatch between Li (110) plane spacing (2.48 Å) and the length of one carbon hexagon ring (2.46 Å) along the graphene zigzag directions is 0.8%, indicating an epitaxial growth of lithium metal.[85] To investigate the Li structure in the confinement of bilayer graphene, Kuehne et al. designed an in-situ electrochemical device consisting of mechanically exfoliated bilayer graphene as the working electrode and a metallic count electrode connected by a Li-ion conducting electrolyte, as shown in Figure 5C.[23] In-situ transmission electron microscopy revealed that Li atoms are arranged in a close-packed order between two graphene sheets, forming a super dense phase with a storage capacity much higher than that expected for LiC_6 structure, consistent with theoretical calculations.[20,23].

Based on the adsorption energy (~1.416 eV for a Li atom) and the cohesive energy of 1.606 eV, the theoretical open circuit voltage (OCV) of Li on graphene can be estimated as −0.19 V,[29] but inconsistent with experimental OCV of Li (~2.25 V) on SLG.[87] To explain the discrepancy, Zhang et al. considered that the interaction between Li and graphene could be strengthened in

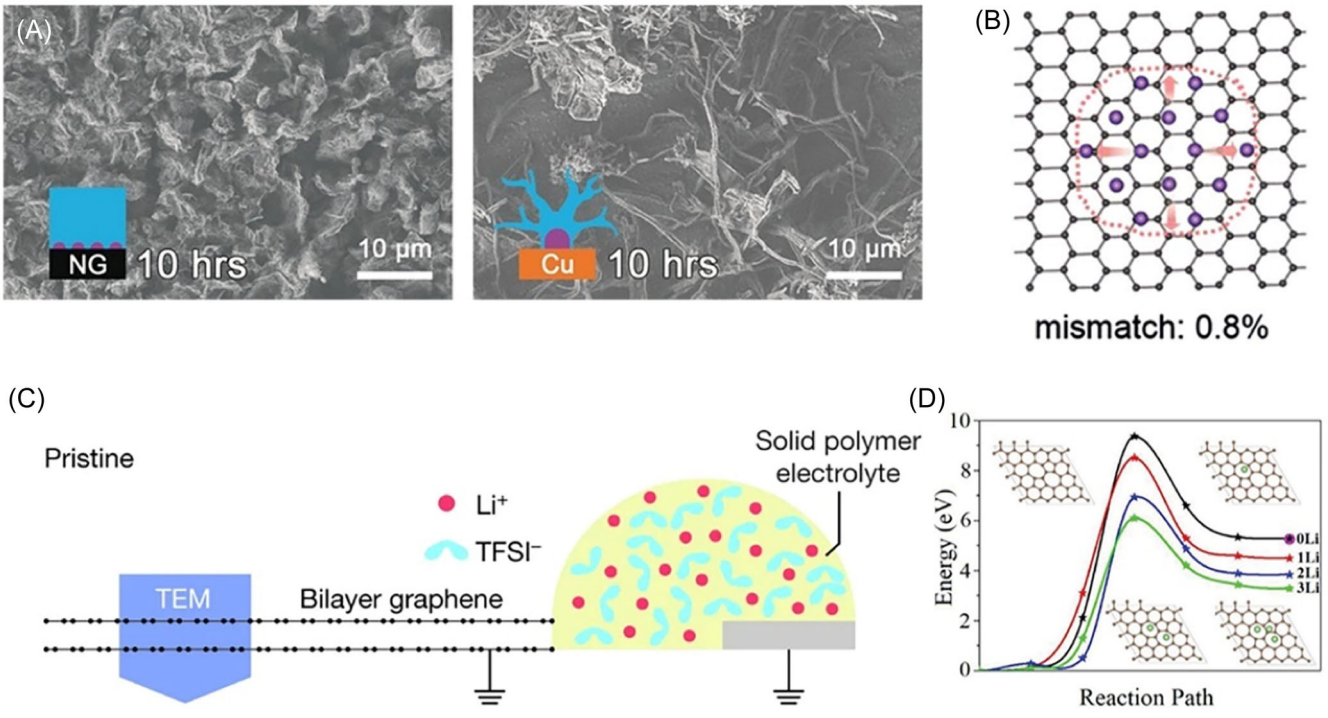

FIGURE 5 (A) Scanning electron microscope images of nitrogen-doped graphene electrode and Cu foil electrode after 0.50 mAh cm^{-2} Li plating.[84] (B) Schematic illustration of Li storage on the graphene with the lattice mismatch between Li (110) plane and graphene.[85] (C) Side view of the in-situ transmission electron microscopy device for Li^+ storage in bilayer graphene.[23] (D) Reaction pathway and formation energy of Stone–Wales defect with different numbers of adsorbed Li atoms.[20] (A) Reproduced with permission.[84] Copyright 2017, Wiley-VCH. (B) Reproduced with permission.[85] Copyright 2020, Wiley-VCH. (C) Reproduced under the terms of the CC-BY Creative Commons Attribution 4.0 International License.[23] Copyright 2018, Springer Nature. (D) Reproduced with permission.[20] Copyright 2019, Wiley-VCH.

disordered graphene, thus improving the Li wettability.[88] To check the stability of SLG for Li adsorption, Ni et al. investigated the Li storage on SLG by in-situ Fourier transform infrared spectroscopy, Raman spectroscopy, and DFT simulations, showing that Li adsorption and the defect formation in graphene promote each other.[20] Consistent with the increased I_D/I_G of Raman spectra during electrochemical cycling, DFT demonstrated that the formation energy and formation barrier of defects decreased with lithium adsorption,[20] as demonstrated in Figure 5D. While the crystal orbital Hamilton population of C–C interactions in the pristine SLG is nearly zero at the Fermi energy (0 eV), an evident antibonding (positive) peak emerges near the Fermi energy when Li adsorbs on the SLG,[20] implying the decreased strength of the C–C bond. That is, Li adsorption may promote the defect formation in graphene.

7 | CONCLUSION AND REMARKS

Graphene provides us with a neat model by ignoring the effects from some complex factors (pores, functionalization, etc.) for studying the EES of carbon electrodes. In the past decade, through the structural regulation, applying ionic gating effect, characterizing ion storage at interface and in confined space, and the understanding of interaction between Li and graphene, the strategies for improving the EES performance of carbon electrodes have been extensively developed.

In practical applications, we have graphene materials with defects and heteroatom doping, beyond nearly unlimited number of structural variants. The precise control of these structural aspects while keeping high SSA and preventing the stacking of graphitic layers remains a challenge, which calls for novel synthetical methods and large-scale molecular dynamics simulations to understand the growth/stacking dynamics. To investigate the impact of solvent and ions on the interface, the development of advanced characterization methods is valuable. The regulation of ion interactions within confined spaces by ion gating effects and nanofluidics and the analysis of their topological structures are some other significant focus of studies. Further tailoring the interlayer space of graphene would be important to understand more deeply on the confinement, where the capacitance could be affected by the distortion and dissolution of hydrated structures, the disruption of Coulombic order, and other complicated interactions between ions and electrode. This involves a combination of in-situ experiments and theoretical simulations to gain insights into ion behavior in these confined environments. Direct observation and associated analysis of the localized nonuniform charge distribution resulting from nonideal and uniform adsorption of ions and solvents molecules on graphene is another critical aspect to be further investigated. The development of experimental characterization techniques with resolutions at the sub-nanometer scale may facilitate this study. We hope these topics would lead us toward better EES devices made from carbon electrode materials.

ACKNOWLEDGMENTS

This work was supported by National Key R&D Program of China (Grant No. 2020YFA0711502), National Natural Science Foundation of China (52273234, 52273239, 52325202).

CONFLICT OF INTEREST STATEMENT

The authors declare no conflict of interest.

ORCID

Yanwu Zhu http://orcid.org/0000-0003-1106-5718

REFERENCES

[1] El-Kady MF, Shao Y, Kaner RB. Graphene for batteries, supercapacitors and beyond. *Nat Rev Mater*. 2016;1:16033.
[2] Raccichini R, Varzi A, Passerini S, Scrosati B. The role of graphene for electrochemical energy storage. *Nat Mater*. 2015;14:271-279.
[3] El-Kady MF, Strong V, Dubin S, Kaner RB. Laser scribing of high-performance and flexible graphene-based electrochemical capacitors. *Science*. 2012;335(6074):1326-1330.
[4] Liu D, Ni K, Ye J, Xie J, Zhu Y, Song L. Tailoring the structure of carbon nanomaterials toward high-end energy applications. *Adv Mater*. 2018;30(48):1802104.
[5] Ye J, Simon P, Zhu Y. Designing ionic channels in novel carbons for electrochemical energy storage. *Natl Sci Rev*. 2020;7(1):191-201.
[6] Shao H, Wu YC, Lin Z, Taberna PL, Simon P. Nanoporous carbon for electrochemical capacitive energy storage. *Chem Soc Rev*. 2020;49(10):3005-3039.
[7] Portet C, Yushin G, Gogotsi Y. Electrochemical performance of carbon onions, nanodiamonds, carbon black and multiwalled nanotubes in electrical double layer capacitors. *Carbon*. 2007;45(13):2511-2518.
[8] Liu WW, Feng YQ, Yan XB, Chen JT, Xue QJ. Superior micro-supercapacitors based on graphene quantum dots. *Adv Funct Mater*. 2013;23(33):4111-4122.
[9] Zhu Y, Murali S, Stoller MD, et al. Carbon-based supercapacitors produced by activation of graphene. *Science*. 2011;332(6037):1537-1541.
[10] Peng C, Yan X-b, Wang R-t, Lang J-w, Ou Y-j, Xue Q-j. Promising activated carbons derived from waste tea-leaves and their application in high performance supercapacitors electrodes. *Electrochim Acta*. 2013;87:401-408.
[11] Rose M, Korenblit Y, Kockrick E, et al. Hierarchical micro- and mesoporous carbide-derived carbon as a high-performance electrode material in supercapacitors. *Small*. 2011;7(8):1108-1117.

[12] Chaikittisilp W, Hu M, Wang H, et al. Nanoporous carbons through direct carbonization of a zeolitic imidazolate framework for supercapacitor electrodes. *Chem Commun*. 2012;48(58):7259-7261.
[13] Jiang XF, Li R, Hu M, et al. Zinc-tiered synthesis of 3D graphene for monolithic electrodes. *Adv Mater*. 2019;31(25): 1901186.
[14] Xia J, Chen F, Li J, Tao N. Measurement of the quantum capacitance of graphene. *Nat Nanotechnol*. 2009;4(8):505-509.
[15] Züttel A, Sudan P, Mauron P, Wenger P. Model for the hydrogen adsorption on carbon nanostructures. *Appl Phys A*. 2004;78(7):941-946.
[16] Murali S, Quarles N, Zhang LL, et al. Volumetric capacitance of compressed activated microwave-expanded graphite oxide (a-MEGO) electrodes. *Nano Energy*. 2013;2(5):764-768.
[17] Ji H, Zhao X, Qiao Z, et al. Capacitance of carbon-based electrical double-layer capacitors. *Nat Commun*. 2017;5:3317.
[18] Li Z, Gadipelli S, Li H, et al. Tuning the interlayer spacing of graphene laminate films for efficient pore utilization towards compact capacitive energy storage. *Nat Energy*. 2020;5:160-168.
[19] Wang D-W, Li F, Wu Z-S, Ren W, Cheng HM. Electrochemical interfacial capacitance in multilayer graphene sheets: dependence on number of stacking layers. *Electrochem Commun*. 2009;11(9):1729-1732.
[20] Ni K, Wang X, Tao Z, et al. In operando probing of lithium-ion storage on single-layer graphene. *Adv Mater*. 2019;31(23):1808091.
[21] Zhu J, Childress AS, Karakaya M, et al. Defect-engineered graphene for high-energy- and high-power-density supercapacitor devices. *Adv Mater*. 2016;28(33):7185-7192.
[22] Ye J, Wu YC, Xu K, et al. Charge storage mechanisms of single-layer graphene in ionic liquid. *J Am Chem Soc*. 2019;141(42):16559-16563.
[23] Kühne M, Börrnert F, Fecher S, et al. Reversible superdense ordering of lithium between two graphene sheets. *Nature*. 2018;564:234-239.
[24] An SJ, Li J, Daniel C, Mohanty D, Nagpure S, Wood DL. The state of understanding of the lithium-ion-battery graphite solid electrolyte interphase (SEI) and its relationship to formation cycling. *Carbon*. 2016;105(28):52-76.
[25] Kaskhedikar NA, Maier J. Lithium storage in carbon nanostructures. *Adv Mater*. 2009;21(25-26):2664-2680.
[26] Dahn JR, Zheng T, Liu Y, Xue JS. Mechanisms for lithium insertion in carbonaceous materials. *Science*. 1995;270(5236): 590-593.
[27] Pollak E, Geng B, Jeon K-J, et al. The interaction of Li^+ with single-layer and few-layer graphene. *Nano Lett*. 2010;10(9): 3386-3388.
[28] Fan X, Zheng WT, Kuo J-L. Adsorption and diffusion of li on pristine and defective graphene. *ACS Appl Mater Interfaces*. 2012;4(5):2432-2438.
[29] Zhou L-J, Hou ZF, Wu L-M. First-principles study of lithium adsorption and diffusion on graphene with point defects. *J Phys Chem C*. 2012;116(41):21780-21787.
[30] Chen J, Han Y, Kong X, et al. The origin of improved electrical double-layer capacitance by inclusion of topological defects and dopants in graphene for supercapacitors. *Angew Chem Int Ed*. 2016;55(44):13822-13827.
[31] Xu J, Tan Z, Zeng W, et al. A hierarchical carbon derived from sponge-tmplated activation of graphene oxide for high-performance supercapacitor electrodes. *Adv Mater*. 2016;28(26): 5222-5228.
[32] Xu Y, Lin Z, Zhong X, et al. Holey graphene frameworks for highly efficient capacitive energy storage. *Nat Commun*. 2014;5(1):4554.
[33] Narayanan R, Yamada H, Karakaya M, Podila R, Rao AM, Bandaru PR. Modulation of the electrostatic and quantum capacitances of few layered graphenes through plasma processing. *Nano Lett*. 2015;15(5):3067-3072.
[34] Radich EJ, Kamat PV. Making graphene holey. gold-nanoparticle-mediated hydroxyl radical attack on reduced graphene oxide. *ACS Nano*. 2013;7(6):5546-5557.
[35] Ramasahayam SK, Nasini UB, Shaikh AU, Viswanathan T. Novel tannin-based Si, P co-doped carbon for supercapacitor applications. *J Power Sources*. 2015;275:835-844.
[36] Wang D-W, Li F, Chen Z-G, Lu GQ, Cheng H-M. Synthesis and electrochemical property of boron-doped mesoporous carbon in supercapacitor. *Chem Mater*. 2008;20(22):7195-7200.
[37] Liu HY, Hou ZF, Hu CH, Yang Y, Zhu ZZ. Electronic and magnetic properties of fluorinated graphene with different coverage of fluorine. *J Phys Chem C*. 2012;116(34):18193-18201.
[38] Qu Y, Ding J, Fu H, Chen H, Peng J. Investigation on tunable electronic properties of semiconducting graphene induced by boron and sulfur doping. *Appl Surf Sci*. 2021;542:148763.
[39] Ghosh S, Barg S, Jeong SM, Ostrikov K. Heteroatom-doped and oxygen-functionalized nanocarbons for high-performance supercapacitors. *Adv Energy Mater*. 2020;10(32):2001239.
[40] Lee Y-H, Chang K-H, Hu C-C. Differentiate the pseudocapacitance and double-layer capacitance contributions for nitrogen-doped reduced graphene oxide in acidic and alkaline electrolytes. *J Power Sources*. 2013;227:300-308.
[41] Pham TV, Kim J-G, Jung JY, et al. High areal capacitance of N-doped graphene synthesized by arc discharge. *Adv Funct Mater*. 2019;29(48):1905511.
[42] Zhao X, Zhang Q, Chen CM, et al. Aromatic sulfide, sulfoxide, and sulfone mediated mesoporous carbon monolith for use in supercapacitor. *Nano Energy*. 2012;1(4):624-630.
[43] Wu Z-S, Tan Y-Z, Zheng S, et al. Bottom-up fabrication of sulfur-doped graphene films derived from sulfur-annulated nanographene for ultrahigh volumetric capacitance micro-supercapacitors. *J Am Chem Soc*. 2017; 139(12):4506-4512.
[44] Sruthi T, Tarafder K. Enhancement of quantum capacitance by chemical modification of graphene supercapacitor electrodes: a study by first principles. *Bull Mater Sci*. 2019;42(6):257.
[45] Barbieri O, Hahn M, Herzog A, Kötz R. Capacitance limits of high surface area activated carbons for double layer capacitors. *Carbon*. 2005;43(6):1303-1310.
[46] Zhong J-H, Liu J-Y, Li Q, et al. Interfacial capacitance of graphene: correlated differential capacitance and in situ electrochemical Raman spectroscopy study. *Electrochim Acta*. 2013;110:754-761.
[47] Ye J, Tan H, Wu S, et al. Direct laser writing of graphene made from chemical vapor deposition for flexible, integratable micro-supercapacitors with ultrahigh power output. *Adv Mater*. 2018;30(27):1801384.

[48] Xiao J, Zhan H, Wang X, et al. Electrolyte gating in graphene-based supercapacitors and its use for probing nanoconfined charging dynamics. *Nat Nanotechnol*. 2020;15:683-689.
[49] He X, Tang N, Gao L, et al. Formation of p-n-p junction with ionic liquid gate in graphene. *Appl Phys Lett*. 2014;104:143102.
[50] Das A, Pisana S, Chakraborty B, et al. Monitoring dopants by Raman scattering in an electrochemically top-gated graphene transistor. *Nat Nanotechnol*. 2008;3(4):210-215.
[51] Mak KF, Lui CH, Shan J, Heinz TF. Observation of an electric-field-induced band gap in bilayer graphene by infrared spectroscopy. *Phys Rev Lett*. 2009;102(25):256405.
[52] Cheng C, Jiang G, Simon GP, Liu JZ, Li D. Low-voltage electrostatic modulation of ion diffusion through layered graphene-based nanoporous membranes. *Nat Nanotechnol*. 2018;13(8):685-690.
[53] Mafra DL, Gava P, Malard LM, et al. Characterizing intrinsic charges in top gated bilayer graphene device by Raman spectroscopy. *Carbon*. 2012;50(10):3435-3439.
[54] McCann E. Asymmetry gap in the electronic band structure of bilayer graphene. *Phys Rev B*. 2006;74(16):161403.
[55] Futamura R, Iiyama T, Takasaki Y, et al. Partial breaking of the Coulombic ordering of ionic liquids confined in carbon nanopores. *Nat Mater*. 2017;16(12):1225-1232.
[56] Tsai W-Y, Taberna P-L, Simon P. Electrochemical quartz crystal microbalance (EQCM) study of ion dynamics in nanoporous carbons. *J Am Chem Soc*. 2014;136(24):8722-8728.
[57] Wu Y-C, Ye J, Jiang G, et al. Electrochemical characterization of single layer graphene/electrolyte interface: effect of solvent on the interfacial capacitance. *Angew Chem Int Ed*. 2021;60(24):13317-13322.
[58] Mao X, Brown P, Červinka C, et al. Self-assembled nanostructures in ionic liquids facilitate charge storage at electrified interfaces. *Nat Mater*. 2019;18(12):1350-1357.
[59] Zhan C, Cerón MR, Hawks SA, et al. Specific ion effects at graphitic interfaces. *Nat Commun*. 2019;10:4858.
[60] Lee AA, Perez-Martinez CS, Smith AM, Perkin S. Under-screening in concentrated electrolytes. *Faraday Discuss*. 2017;199:239-259.
[61] Fedorov MV, Kornyshev AA. Ionic liquids at electrified interfaces. *Chem Rev*. 2014;114(5):2978-3036.
[62] Fedorov MV, Georgi N, Kornyshev AA. Double layer in ionic liquids: the nature of the camel shape of capacitance. *Electrochem Commun*. 2010;12(2):296-299.
[63] Georgi N, Kornyshev AA, Fedorov MV. The anatomy of the double layer and capacitance in ionic liquids with anisotropic ions: electrostriction vs. lattice saturation. *J Electroanal Chem*. 2010;649(1):261-267.
[64] Chen K, Song S, Liu F, Xue D. Structural design of graphene for use in electrochemical energy storage devices. *Chem Soc Rev*. 2015;44(17):6230-6257.
[65] Yang H, Yang J, Bo Z, et al. Kinetic-dominated charging mechanism within representative aqueous electrolyte-based electric double-layer capacitors. *J Phys Chem Lett*. 2017;8(15):3703-3710.
[66] Marcus Y. Effect of ions on the structure of water: structure making and breaking. *Chem Rev*. 2009;109(3):1346-1370.
[67] Salitra G, Soffer A, Eliad L, Cohen Y, Aurbach D. Carbon electrodes for double-layer capacitors I. Relations between ion and pore dimensions. *J Electrochem Soc*. 2000;147(7):2486-2493.
[68] Lin C, Ritter JA, Popov BN. Correlation of double-layer capacitance with the pore structure of sol-gel derived carbon xerogels. *J Electrochem Soc*. 1999;146(10):3639-3643.
[69] Endo M, Kim YJ, Takeda T, et al. Poly(vinylidene chloride)-based carbon as an electrode material for high power capacitors with an aqueous electrolyte. *J Electrochem Soc*. 2001;148(10):A1135.
[70] Galhena DTL, Bayer BC, Hofmann S, Amaratunga GAJ. Understanding capacitance variation in sub-nanometer pores by in situ tuning of interlayer constrictions. *ACS Nano*. 2016;10(1):747-754.
[71] Schoch RB, Han J, Renaud P. Transport phenomena in nanofluidics. *Rev Mod Phys*. 2008;80(3):839-883.
[72] Koltonow AR, Huang J. Two-dimensional nanofluidics. *Science*. 2016;351(6280):1395-1396.
[73] Cheng C, Jiang G, Garvey CJ, et al. Ion transport in complex layered graphene-based membranes with tuneable interlayer spacing. *Sci Adv*. 2016;2(2):e1501272.
[74] Nair RR, Wu HA, Jayaram PN, Grigorieva IV, Geim AK. Unimpeded permeation of water through helium-leak–tight graphene-based membranes. *Science*. 2012;335(6067):442-444.
[75] Liu H, Wang H, Zhang X. Facile fabrication of freestanding ultrathin reduced graphene oxide membranes for water purification. *Adv Mater*. 2015;27(2):249-254.
[76] Hung W-S, Tsou C-H, De Guzman M, et al. Cross-linking with diamine monomers to prepare composite graphene oxide-framework membranes with varying d-spacing. *Chem Mater*. 2014;26(9):2983-2990.
[77] Abraham J, Vasu KS, Williams CD, et al. Tunable sieving of ions using graphene oxide membranes. *Nat Nanotechnol*. 2017;12(6):546-550.
[78] Chen L, Shi G, Shen J, et al. Ion sieving in graphene oxide membranes via cationic control of interlayer spacing. *Nature*. 2017;550:380-383.
[79] Esfandiar A, Radha B, Wang FC, et al. Size effect in ion transport through angstrom-scale slits. *Science*. 2017;358(6362):511-513.
[80] Kühne M, Paolucci F, Popovic J, Ostrovsky PM, Maier J, Smet JH. Ultrafast lithium diffusion in bilayer graphene. *Nat Nanotechnol*. 2017;12(9):895-900.
[81] Yao F, Güneş F, Ta HQ, et al. Diffusion mechanism of lithium ion through basal plane of layered. *J Am Chem Soc*. 2012;134(20):8646-8654.
[82] Ren F, Peng Z, Wang M, et al. Over-potential induced Li/Na filtrated depositions using stacked graphene coating on copper scaffold. *Energy Stor Mater*. 2019;16:364-373.
[83] Chen X, Chen X-R, Hou T-Z, et al. Lithiophilicity chemistry of heteroatom-doped carbon to guide uniform lithium nucleation in lithium metal anodes. *Sci Adv*. 2019;5(2):eaau7728.
[84] Zhang R, Chen X-R, Chen X, et al. Lithiophilic sites in doped graphene guide uniform lithium nucleation for dendrite-free lithium metal anodes. *Angew Chem Int Ed*. 2017;56(27):7764-7768.
[85] Li N, Zhang K, Xie K, et al. Reduced-graphene-oxide-guided directional growth of planar lithium layers. *Adv Mater*. 2020;32(7):1907079.

[86] Yan K, Lu Z, Lee H-W, et al. Selective deposition and stable encapsulation of lithium through heterogeneous seeded growth. *Nat Energy*. 2016;1(3):16010.
[87] Wei D, Astley MR, Harris N, White R, Ryhänen T, Kivioja J. Graphene nanoarchitecture in batteries. *Nanoscale*. 2014; 6(16):9536-9540.
[88] Zhang R, Cheng X-B, Zhao C-Z, et al. Conductive nanostructured scaffolds render low local current density to inhibit lithium dendrite growth. *Adv Mater*. 2016;28(11):2155-2162.

AUTHOR BIOGRAPHIES

Minghao Guo is a PhD candidate at the Department of Materials Science and Engineering, University of Science and Technology of China. He received his BS from School of Materials Science and Engineering, Wuhan University of Technology in 2019. His research interests are understanding structural evolution and exploring application of carbon material by simulations.

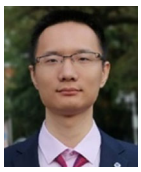

Kun Ni is an associate research fellow at the Department of Materials Science and Engineering, University of Science and Technology of China. He received his BS and PhD from University of Science and Technology of China in 2014 and 2019, respectively. He finished postdoctoral research at University of Science and Technology of China in 2021. His research interests are the structural design and interface modulation of carbon materials toward high-performance low-cost energy storage, electro-catalytic, mechanical and thermal dissipation applications by using density functional theory simulations, accompanied by machine-learning methods.

Yanwu Zhu is a professor at the Department of Materials Science and Engineering, University of Science and Technology of China. In 2007, he received his PhD degree from Department of Physics, National University of Singapore. Before his current position, he worked as a postdoctoral researcher at National University of Singapore and the University of Texas at Austin. His research interest includes the synthesis of novel carbon nanomaterials and their application in energy storage and conversion.

How to cite this article: Guo M, Ni K, Zhu Y. Storage dynamics of ions on graphene. *Interdiscip Mater*. 2024;3:189-202. doi:10.1002/idm2.12146